T. L. Yip

T. Sahoo

A. T. Chwang
Fellow ASME

Department of Mechanical Engineering,
The University of Hong Kong,
Pokfulam Road,
Hong Kong

Wave Oscillation in a Circular Harbor With Porous Wall

The wave resonance in a circular harbor surrounded by a porous seawall is analyzed. Matching the velocity and pressure along the porous seawall and the harbor entrance, the full solution is obtained. The resonance condition is found to depend on the wave frequency, the complex porous-effect parameter and the internal dimension of the porous seawall. The oscillation characteristics are analyzed in different cases. The condition for natural oscillation is derived by studying the wave resonance in a closed circular harbor surrounded by a porous seawall. [DOI: 10.1115/1.1379955]

1 Introduction

In the last decade, there has been a significant change in the nature of harbor traffic in Hong Kong, which results in the deterioration of wave conditions in Victoria Harbor. As a result, the dynamic and mooring forces acting on ships and docks are seriously affected by the high wave oscillation and in turn create serious problems to different marine structures, affecting loading and unloading of cargoes. As a means to dissipate wave energy, a porous seawall is introduced inside an existing harbor, which will reduce the wave oscillation and improve the general wave climate.

The vertical-wall harbors are widely used for their simple design and construction. In the presence of waves, a vertical harbor wall reflects most of the wave energy incident on it. With strong harbor oscillations, vertical walls are subjected to large wave forces. Recently, permeable breakwaters, detached breakwaters, and submerged breakwaters have received much attention and their capability to dissipate wave energy is widely studied. Some of the energy-dissipating breakwaters are being tested in harbors ([1,2]).

On the other hand, wave agitation in harbor due to an incoming wave of a particular frequency may last for a long time. This agitation leads to a resonant state and is the cause of extremely high wave oscillations inside the harbor. The dynamic and mooring forces acting on marine structures are increased during this high oscillation which usually create serious problems to loading and unloading of cargoes. Thus, during the harbor planning, measures should be taken to avoid such harbor resonance. There are two kinds of oscillations existing in a harbor, one is the free oscillation and the other forced oscillation. Lamb [3] analyzed the effect of free oscillation in closed rectangular, circular, and elliptical basins. McNown [4] investigated the forced oscillation in a circular harbor having a narrow opening. In a rectangular harbor, the effect of forced oscillation was analyzed by Kravtchnenko and McNown [5]. Further study on harbor resonance was done by Miles and Munk [6], LeMehaute [7] and Ippen and Goda [8]. Miles and Munk [6] found that the wider the harbor mouth, the smaller the amplitude of the resonant oscillation which is contradictory to the fact that less wave energy will be transmitted to the harbor through a smaller opening. This phenomenon was known as the harbor paradox. Lee [9] considered rectangular and circular harbors with their openings located on a straight coastline while Mei and Petroni [10] dealt with a circular harbor protruding halfway into the open sea. To deal with arbitrary harbor configuration, Hwang and Tuck [11] and Lee [9] developed integral equation methods while Mei and Chen [12] provided a hybrid element method. Numerical studies for harbors of arbitrary geometry have also been verified by field and experimental data (e.g. [9,11]). Recently, certain amount of numerical work is available to include the reflectivity of the harbor wall ([13,14]). However, because of the deficiency of numerical methods, the results can only represent special conditions, not the general relationship between the reflectivity and the harbor oscillation.

In recent times, porous breakwaters are being constructed for dissipating wave energy in order to reduce the hydrodynamic forces on breakwaters. With the assumption of Darcy's law, Sollitt and Cross [15] and Chwang [16] separately developed models to study the flow past porous structures. These methods were unified and combined by Yu and Chwang [17] to become the most acceptable one in the recent literature of flow past porous structures. Yu and Chwang [17] studied the problem of wave resonance in a harbor with a porous breakwater. It is observed that a porous breakwater can reduce the amplitude of resonant frequency significantly. A small but finite permeability of the breakwater is found to be optimal to diminish the resonant oscillation.

In the present paper, we investigate the problem of wave resonance in a circular basin surrounded by a porous breakwater. The basin has an entrance located on a straight coastline. As a particular case, the wave resonance in a closed circular basin surrounded by a permeable breakwater is analyzed. Matching the velocity as well as the pressure along the porous seawall and the harbor entrance, the full solution is obtained and the resonance condition is derived. The effect of the porous-effect parameter and the position of the breakwater on wave oscillation are analyzed. The present work should be useful in future harbor design and modifications.

2 Formulation of the Problem

The problem under consideration is three dimensional in nature and is studied in a cylindrical coordinate system with uniform depth h. The opening of the harbor is along the coastline at a distance $b\cos\varepsilon$ from the center of the harbor with 2ε being the opening angle of the harbor (see Fig. 1). The circular harbor is of radius b with an inner permeable circular wall of radius a. Assuming that the fluid is inviscid and incompressible and its motion irrotational, we can define a velocity potential $\Phi(r,\theta,z,t)$ which satisfies the Laplace equation. Assuming the motion is simple harmonic in time, we can express Φ as $\Phi(r,\theta,z,t) = \mathrm{Re}[\phi(r,\theta,z)e^{-i\omega t}]$ with ω being the angular frequency. The fluid domain is divided into three regions: (i) the open sea region, (ii) the region between the porous wall and the solid harbor wall and (iii) the inner harbor region surrounded by the porous wall. ϕ_j $(j=1,2,3)$ denotes the velocity potential in region j. The spatial velocity potential ϕ satisfies the Laplace equation

Contributed by the Applied Mechanics Division of THE AMERICAN SOCIETY OF MECHANICAL ENGINEERS for publication in the ASME JOURNAL OF APPLIED MECHANICS. Manuscript received by the ASME Applied Mechanics Division, June 24, 2000; final revision, Sept. 26, 2000. Associate Editor: D. A. Siginer. Discussion on the paper should be addressed to the Editor, Prof. Lewis T. Wheeler, Department of Mechanical Engineering, University of Houston, Houston, TX 77204-4792, and will be accepted until four months after final publication of the paper itself in the ASME JOURNAL OF APPLIED MECHANICS.

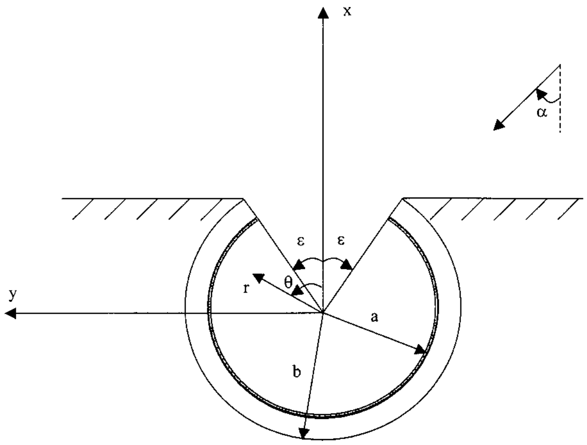

Fig. 1 Schematic diagram of a circular harbor

$$\frac{1}{r}\frac{\partial}{\partial r}\left(r\frac{\partial\phi}{\partial r}\right)+\frac{1}{r^2}\frac{\partial^2\phi}{\partial\theta^2}+\frac{\partial^2\phi}{\partial z^2}=0. \tag{1}$$

The free surface boundary condition is given by

$$\frac{\partial\phi}{\partial z}-\frac{\omega^2}{g}\phi=0 \quad \text{at } z=0, \tag{2}$$

where g is the gravitational constant. The bottom boundary condition is given by

$$\frac{\partial\phi}{\partial z}=0 \quad \text{at } z=-h. \tag{3}$$

As r tends to infinity, the scattered wave potential ϕ_s satisfies the radiation condition

$$\sqrt{r}\left(\frac{\partial\phi_s}{\partial r}-ik_0\phi_s\right)\rightarrow 0, \quad \text{as } r\rightarrow\infty, \tag{4}$$

where k_0 is the wave number of the incoming progressive wave. Along the straight coastline, the velocity potential satisfies the condition

$$\frac{\partial\phi}{\partial x}=0 \quad \text{at } x=b\cos\varepsilon. \tag{5}$$

The continuity of pressure along the harbor opening requires

$$\phi_1=\phi_2 \quad \text{on} \quad r=b, \quad -\varepsilon<\theta<\varepsilon. \tag{6}$$

The vanishing of velocity along the impermeable harbor wall and the continuity of velocity along the opening is given by

$$\phi_{2r}=\begin{cases}0, & \text{at } r=b, \quad \varepsilon<\theta<2\pi-\varepsilon,\\ \phi_{1r} & \text{at } r=b, \quad -\varepsilon<\theta<\varepsilon.\end{cases} \tag{7}$$

The condition along the porous wall and the opening of the porous wall is given by

$$ik_0G(\phi_3-\phi_2)=\begin{cases}0, & \text{at } r=a, \quad -\varepsilon<\theta<\varepsilon,\\ \phi_{3r}, & \text{at } r=a, \quad \varepsilon<\theta<2\pi-\varepsilon,\end{cases} \tag{8}$$

where G is the porous-effect parameter or the Chwang parameter ([18]), which is different from the Chwang's wave-effect parameter ([19]). The porous-effect parameter G is a complex number with non-negative real and imaginary parts. The real part of G represents the resistance effect of a porous medium against the flow. The imaginary part of G denotes the inertia effect of fluids in the porous medium.

Finally, the continuity of velocity along the opening of the porous wall is given by

$$\frac{\partial\phi_2}{\partial r}=\frac{\partial\phi_3}{\partial r} \quad \text{on} \quad r=a, \quad -\varepsilon<\theta<\varepsilon. \tag{9}$$

3 The Method of Solution

The velocity potential for the open sea region is the superposition of plane waves with the coastline reflection in the absence of the harbor, ϕ_I, and the scattered wave ϕ_s due to the presence of the harbor,

$$\begin{aligned}\phi_I&=A_I\{e^{-ik_0[-(x-b\cos\varepsilon)\cos\alpha+y\sin\alpha]}\\&\quad+e^{ik_0[(x-b\cos\varepsilon)\cos\alpha+y\sin\alpha]}\}f_0(z)\\&=A_If_0(z)\sum_{m=0}^{\infty}\beta_m\{\Omega_m^c\psi_m^c+\Omega_m^s\psi_m^s\}J_m(k_0r),\end{aligned} \tag{10}$$

$$\begin{aligned}\phi_S=\sum_{m=0}^{\infty}\Bigg[&(A_{m0}^c\psi_m^c+A_{m0}^s\psi_m^s)\frac{H_m(k_0r)}{H_m'(k_0b)}f_0(z)\\&+\sum_{n=1}^{\infty}(A_{mn}^c\psi_m^c+A_{mn}^s\psi_m^s)\frac{K_m(k_nr)}{K_m'(k_nb)}f_n(z)\Bigg],\end{aligned} \tag{11}$$

where $f_0(z)=\cosh k_0(h+z)/\cosh k_0h$, $f_n(z)=\cos k_n(h+z)$, $A_I=gH/2\omega$, α is the incident wave angle, H is the incident wave height, $\beta_0=1$, $\beta_n=2$, $(n=1,2,3\ldots)$, $J_m(\cdot)$ is the Bessel function of the first kind, $H_m(\cdot)$ is the Hankel function of the first kind, $K_m(\cdot)$ is the modified Bessel function of the second kind, A_{mn}^c, A_{mn}^s are unknown constants to be determined,

$$\psi_m^c=\cos m\theta, \quad \psi_m^s=\sin m\theta,$$

$$\Omega_m^c=[(-i)^m e^{ik_0b\cos\varepsilon\cos\alpha}+(i)^m e^{-ik_0b\cos\varepsilon\cos\alpha}]\cos m\alpha,$$

$$\Omega_m^s=[-(-i)^m e^{ik_0b\cos\varepsilon\cos\alpha}+(i)^m e^{-ik_0b\cos\varepsilon\cos\alpha}]\sin m\alpha.$$

Superscripts c and s represent the terms associated with ψ_m^c and ψ_m^s, respectively. In (4) and (11), wave numbers $k_n(n=0,1,2,\ldots)$ satisfy the dispersion relations

$$\omega^2=gk_0\tanh k_0h=-gk_n\tan k_nh. \tag{12}$$

Hence, in region 1,

$$\phi_1=\phi_I+\phi_S. \tag{13}$$

The velocity potentials $\phi_j(j=2,3)$ are of the form

$$\begin{aligned}\phi_2=\sum_{m=0}^{\infty}\Bigg\{\Bigg[&(B_{m0}^c\psi_m^c+B_{m0}^s\psi_m^s)\frac{J_m(k_0r)}{J_m'(k_0b)}+(C_{m0}^c\psi_m^c\\&+C_{m0}^s\psi_m^s)\frac{Y_m(k_0r)}{Y_m'(k_0b)}\Bigg]f_0(z)+\sum_{n=1}^{\infty}\Bigg[(B_{mn}^c\psi_m^c+B_{mn}^s\psi_m^s)\\&\times\frac{I_m(k_nr)}{I_m'(k_nb)}+(C_{mn}^c\psi_m^c+C_{mn}^s\psi_m^s)\frac{K_m(k_nr)}{K_m'(k_nb)}\Bigg]f_n(z)\Bigg\},\end{aligned} \tag{14}$$

$$\begin{aligned}\phi_3=\sum_{m=0}^{\infty}\Bigg\{&(D_{m0}^c\psi_m^c+D_{m0}^s\psi_m^s)\frac{J_m(k_0r)}{J_m'(k_0a)}f_0(z)\\&+\sum_{n=1}^{\infty}(D_{mn}^c\psi_m^c+D_{mn}^s\psi_m^s)\frac{I_m(k_nr)}{I_m'(k_na)}f_n(z)\Bigg\},\end{aligned} \tag{15}$$

where B_{mn}^p, C_{mn}^p, D_{mn}^p $(p=c,s;m,n=0,1,2,\ldots)$ are unknown constants to be determined, $I_m(\cdot)$ is the modified Bessel function of the first kind, and $Y_m(\cdot)$ is the Bessel function of the second kind.

From (6), (7), (13), (14) and the orthogonality of f_n and ψ_m^p $(p=c,s)$, we have

$$\sum_{j=0}^{\infty}\left\{B_{j0}^{p}\frac{J_j(k_0b)}{J_j'(k_0b)}+C_{j0}^{p}\frac{Y_j(k_0b)}{Y_j'(k_0b)}-A_{j0}^{p}\frac{H_j(k_0b)}{H_j'(k_0b)}\right.$$
$$\left.-A_I\beta_j\Omega_j^p\psi_j^pJ_j(k_0b)\right\}e_{jm}^p=0,\quad (p=c,s;m=0,1,2,\ldots),\tag{16}$$

$$\sum_{j=0}^{\infty}\left\{B_{jn}^{p}\frac{I_j(k_nb)}{I_j'(k_nb)}+C_{jn}^{p}\frac{K_j(k_nb)}{K_j'(k_nb)}-A_{jn}^{p}\frac{K_j(k_nb)}{K_j'(k_nb)}\right\}e_{jm}^p=0,$$
$$(p=c,s;n=1,2,\ldots;m=0,1,2,\ldots),\tag{17}$$

$$(B_{m0}^p+C_{m0}^p)d_m^p=\sum_{j=0}^{\infty}[A_I\beta_j\Omega_j^pJ_m'(k_0b)+A_{m0}^p]e_{jm}^p$$
$$(m=0,1,2,\ldots),\tag{18}$$

$$(B_{mn}^p+C_{mn}^p)d_m^p=\sum_{j=0}^{\infty}e_{mj}^pA_{jn}\quad (n=1,2,3,\ldots;m=0,1,2,\ldots),\tag{19}$$

where

$$d_m^p=\int_0^{2\pi}[\psi_m^p]^2d\theta,\ \ e_{jm}^p=\int_{-\varepsilon}^{\varepsilon}\psi_j^p\psi_m^pd\theta.$$

From (8), (9), (14), (15) and the orthogonality of f_n and $\psi_m^p(p=c,s)$, we obtain

$$ik_0G\left[\frac{J_m(k_0a)}{J_m'(k_0a)}D_{m0}^p-\left(\frac{J_m(k_0a)}{J_m'(k_0b)}B_{m0}^p+\frac{Y_m(k_0a)}{Y_m'(k_0b)}C_{m0}^p\right)\right]d_m^p$$
$$=\sum_{j=0}^{\infty}k_0D_{j0}^pf_{mj}^p\quad (m=0,1,2,\ldots),\tag{20}$$

$$ik_0G\left[\frac{I_m(k_na)}{I_m'(k_na)}D_{mn}^p-\left(\frac{K_m(k_na)}{K_m'(k_nb)}B_{mn}^p+\frac{I_m(k_na)}{I_m'(k_nb)}C_{mn}^p\right)\right]d_m^p$$
$$=\sum_{j=0}^{\infty}k_nD_{jn}^pf_{mj}^p\quad (n=1,2,3,\ldots;m=0,1,2,\ldots),\tag{21}$$

where

$$f_{mj}^p=\int_{\varepsilon}^{2\pi-\varepsilon}\psi_m^p\psi_j^pd\theta.\tag{22}$$

$$\frac{J_m'(k_0a)}{J_m'(k_0b)}B_{m0}^p+\frac{Y_m'(k_0a)}{Y_m'(k_0b)}C_{m0}^p=D_{m0}^p\quad (p=c,s;m=0,1,2,\ldots),$$
$$\frac{I_m'(k_na)}{I_m'(k_nb)}B_{mn}^p+\frac{K_m'(k_na)}{K_m'(k_nb)}C_{mn}^p=D_{mn}^p$$
$$(p=c,s;m=0,1,2,\ldots;n=1,2,3,\ldots).\tag{23}$$

The system of equations (16)–(23) can be solved to obtain the complete solution.

4 Oscillation in a Closed Basin

In such a case, we have $\varepsilon=0$. The velocity potential ϕ_1 will not be taken into account. Without loss of generality, the velocity potentials are

$$\phi_2=\sum_{m=0}^{\infty}\left\{\left[B_{m0}\frac{J_m(k_0r)}{J_m'(k_0b)}+C_{m0}\frac{Y_m(k_0r)}{Y_m'(k_0b)}\right]f_0(z)\right.$$
$$\left.+\sum_{n=1}^{\infty}\left[B_{mn}\frac{I_m(k_nr)}{I_m'(k_nb)}+C_{mn}\frac{K_m(k_nr)}{K_m'(k_nb)}\right]f_n(z)\right\}\cos m\theta,\tag{24}$$

$$\phi_3=\sum_{m=0}^{\infty}\left\{D_{m0}\frac{J_m(k_0r)}{J_m'(k_0a)}f_0(z)+\sum_{n=1}^{\infty}D_{mn}\frac{I_m(k_nr)}{I_m'(k_na)}f_n(z)\right\}\cos m\theta.\tag{25}$$

It may be noted that $k_n\,(n=0,1,2,\ldots)$ are related to the angular frequency of the free oscillation of the harbor. In this case, we have $\phi_{2r}=0$ on $r=b$ which gives

$$B_{mn}=-C_{mn}\quad (m,n=0,1,2,\ldots).\tag{26}$$

Condition (8) along the permeable wall becomes

$$\frac{\partial\phi_2}{\partial r}=\frac{\partial\phi_3}{\partial r}=ik_0G(\phi_3-\phi_2)\quad \text{at } r=a(j=2,3).\tag{27}$$

The orthogonality of $f_n\,(n=0,1,2,\ldots)$ and $\cos m\theta$ leads to

$$\left[\frac{J_m'(k_0a)}{J_m'(k_0b)}-\frac{Y_m'(k_0a)}{Y_m'(k_0b)}\right]B_{m0}=D_{m0}\quad (m=0,1,2,\ldots),\tag{28}$$

$$\left[\frac{I_m'(k_na)}{I_m'(k_nb)}-\frac{K_m'(k_na)}{K_m'(k_nb)}\right]B_{mn}=D_{mn}$$
$$(n=1,2,3,\ldots;m=0,1,2,\ldots),\tag{29}$$

$$ik_0G\left[\frac{J_m(k_0a)}{J_m'(k_0a)}D_{m0}-\left(\frac{J_m(k_0a)}{J_m'(k_0b)}-\frac{Y_m(k_0a)}{Y_m'(k_0b)}\right)B_{m0}\right]=k_0D_{m0}$$
$$(m=0,1,2,\ldots),\tag{30}$$

$$ik_0G\left[\frac{I_m(k_na)}{I_m'(k_na)}D_{mn}-\left(\frac{I_m(k_na)}{I_m'(k_nb)}-\frac{K_m(k_na)}{K_m'(k_nb)}\right)B_{mn}\right]=k_nD_{mn}$$
$$(n=1,2,3,\ldots;m=0,1,2,\ldots).\tag{31}$$

From Eq. (28)–(31), we derive the resonance conditions relating the porous-effect parameter, the radius of the circular basin, the permeable wall and the wave number of the progressive wave mode as

$$iG\left[\frac{J_m(k_0a)}{J_m'(k_0a)}\left(\frac{J_m'(k_0a)}{J_m'(k_0b)}-\frac{Y_m'(k_0a)}{Y_m'(k_0b)}\right)-\left(\frac{J_m(k_0a)}{J_m'(k_0b)}-\frac{Y_m(k_0a)}{Y_m'(k_0b)}\right)\right]$$
$$=\left(\frac{J_m'(k_0a)}{J_m'(k_0b)}-\frac{Y_m'(k_0a)}{Y_m'(k_0b)}\right)\quad (m=0,1,2,\ldots),\tag{32}$$

$$ik_0G\left[\frac{I_m(k_na)}{I_m'(k_na)}\left(\frac{I_m'(k_na)}{I_m'(k_nb)}-\frac{K_m'(k_na)}{K_m'(k_nb)}\right)-\left(\frac{I_m(k_na)}{I_m'(k_nb)}-\frac{K_m(k_na)}{K_m'(k_nb)}\right)\right]$$
$$=k_n\left(\frac{I_m'(k_na)}{I_m'(k_nb)}-\frac{K_m'(k_na)}{K_m'(k_nb)}\right)\quad (n=1,2,3,\ldots;m=0,1,2,\ldots).\tag{33}$$

From (32) and (33), it is obvious that there is no real root for real G. Hence, there is no steady oscillation in a circular harbor with a permeable wall, which is similar to the observation of Yu and Chwang [17].

From (32) after rearrangement, we have

$$\frac{J_m'(k_0a)}{J_m'(k_0b)Y_m'(k_0a)}-\frac{iGJ_m(k_0a)-J_m'(k_0a)}{iGY_m(k_0a)J_m'(k_0b)-Y_m'(k_0b)J_m'(k_0a)}=0.\tag{34}$$

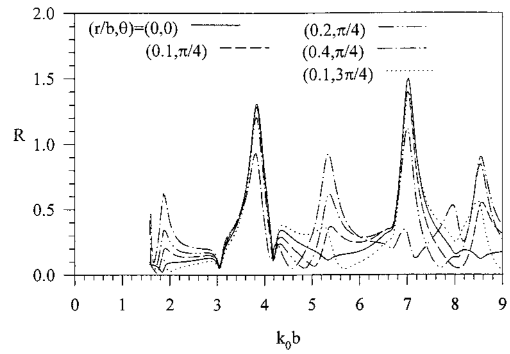

Fig. 3 Variation of amplification factor R versus wave number k_0b at different locations with α=0 deg, b/h=0.75, 2ε=10 deg, G=1, and $(b-a)/\lambda=0.25$

When $G=0$, the inner permeable wall behaves like a solid wall and we have a closed circular region and another annular region. From (34),

$$J'_m(k_0a)=0 \quad (m=0,1,2,\ldots) \tag{35a}$$

or

$$J'_m(k_0a)Y'_m(k_0b)-J'_m(k_0b)Y'_m(k_0a)=0 \quad (m=0,1,2,\ldots). \tag{35b}$$

The solution of (35*a*) represents the wave modes due to a closed circular basin of radius a, while the solution of (35*b*) represents the wave modes inside the closed annular basin with inner and outer radii a and b, respectively. On the other hand, as $G\to\infty$, the permeable wall becomes transparent to the fluid and the resonance is due to the free oscillation of a closed circular basin of radius b. In such a case, from (34), we derive

$$J'_m(k_0b)=0 \quad (m=0,1,2,\ldots). \tag{36}$$

5 Discussion

The amplification factor R which is a measure of wave oscillation inside the harbor is defined as

$$R=\left|\frac{\phi_3(r,\theta,0)}{A_I}\right|. \tag{37}$$

In the two-dimensional analysis of Chwang and Dong [20], when the porous-effect parameter $G=1$ and gap length $(b-a)=(2n+1)\lambda/4$, the reflection coefficient vanishes and the phenomenon of wave trapping takes place. From Yip and Chwang [21] it was noted that the curves for complex values of G are of similar shape as those for real values. To avoid repetition of similar results which have been investigated before, the curves for complex values of G are not presented in the present paper.

Figure 2 shows the variation of amplification factor R at the center versus wave number k_0b for different values of the porous-effect parameter G. As $0<a<b$, we must have $0<2\pi(b-a)/\lambda<k_0b$. The amplification factor R increases generally as G increases. As G increases, the porous wall becomes transparent to the fluid and most of the wave energy is reflected back by the vertical harbor wall with an increase in the wave oscillation and thus an increase in the amplification factor. However, it should be noted that when $G=1$, the wave dissipation is maximum (see [17,20]) and in the process the wave resonance is minimum. The amplification factor R attains maxima for certain values of the wave number irrespective of the porous-effect parameter. The real porous-effect parameter only reduces the amplification factor without affecting the wave number.

In Fig. 3, the amplification factor R is plotted versus wave number k_0b at different locations in the inner region of the harbor. The amplification factor R attains its maximum value at different locations for different wave number k_0b. Generally speaking, the wave amplification is large near the center compared to a point towards the harbor wall. It should be noted that, for normal incidence $\alpha=0$ deg, the wave condition inside the harbor is symmetric with respect to $\theta=0$ deg.

Figure 4 shows the variation of amplification factor R at the harbor center versus the gap length $(b-a)/\lambda$ for different values of the porous-effect parameter G. The two-dimensional result of Chwang and Dong [20] showed that the wave dissipation is maximum at $(b-a)/\lambda=0.25$, and the amount of dissipated energy depends on the porous-effect parameter G. The same phenomenon was observed later by Fugazza and Natale [22] and Suh and Park [23] although their analyses were different. Similar phenomemon is observed in the case of a circular harbor. However, the wave dissipation is more sensitive in the two-dimensional case ([20]) near $(b-a)/\lambda=0.25$, while in the present case of a circular harbor, large dissipation occurs at a wider range of $(b-a)/\lambda$ near 0.25. It should be noted that the wave incidence at the porous wall is not always normal but varying along the porous wall. In general, the incidence angle along the porous wall is very difficult to predict for three-dimensional cases. As shown in Fig. 4, the wave is dissipated most for a moderate value of G. Larger G represents a more porous wall and less wave energy is dissipated. As $G\to\infty$, the porous wall becomes transparent to the fluid and no dissipation occurs.

Figure 5 shows the variation of amplification factor R at the harbor center versus harbor opening 2ε for different values of the porous-effect parameter G. When the opening of the harbor vanishes, the amplification factor R becomes zero, as no wave is allowed to enter the harbor. A large amplification factor R is observed at moderate values of opening 2ε, similar to "the harbor

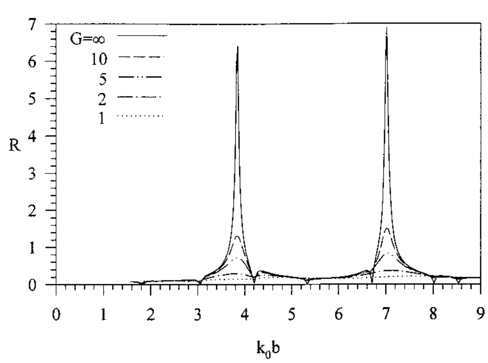

Fig. 2 Variation of amplification factor R at the center versus wave number k_0b for different values of G with α=0 deg, b/h=0.75, 2ε=10 deg, and $(b-a)/\lambda=0.25$

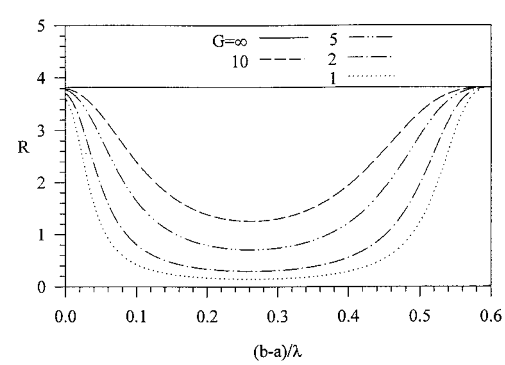

Fig. 4 Variation of amplification factor R at the center versus $(b-a)/\lambda$ for different values of G with α=0 deg , b/h=0.75, 2ε=10 deg, and k_0b=3.8

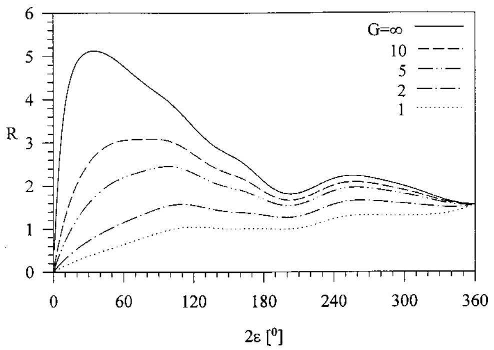

Fig. 5 Variation of amplification factor R at the center versus harbor opening 2ε for different values of G with $\alpha=0$ deg, $b/h=0.75$, $k_0b=3.8$, and $(b-a)/\lambda=0.25$

paradox," and the harbor oscillation decreases generally as the opening 2ε further increases. There is a sharp decrease in the amplification factor R with a decrease of the porous-effect parameter G. There is a shift in the maximum of the amplification factor as G decreases and the opening angle of the harbor increases. When the harbor becomes a point and only the straight coast remains, all curves come to the same limiting value.

Figure 6 illustrates the variation of amplification factor R at the center versus incidence angle α of incident waves. Because of the symmetry of the problem, the curves are symmetric with respect to $\alpha=0$ deg. The increase of incidence angle α allows less wave energy to transmit through the opening to the harbor. Thus, the normal incidence allows the most wave energy into the harbor. The amplification factor R tends to fixed values as incidence angle α approaches ± 90 deg.

Just as a remark to the current practice in numerical computation, the partially reflective boundary condition

$$\frac{\partial \phi}{\partial n}=k_0\frac{1-K_r}{1+K_r}\phi,$$

where K_r is the normal reflection coefficient at the boundary, is widely used by prescribing K_r as a constant. However, K_r depends on the wave number and incidence direction and no analytical solution can be obtained if the partially reflective boundary condition is applied in this problem. To sum up, the above analyses are for a harbor of circular geometry. As previous analyses have demonstrated, the harbor geometry is a critical factor to harbor oscillations.

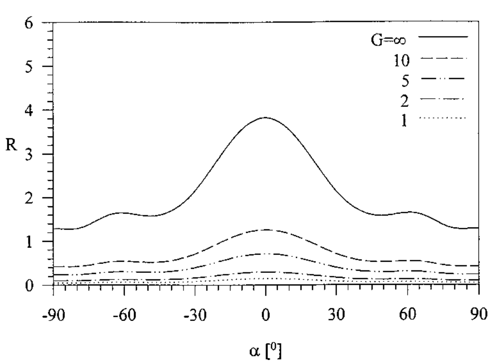

Fig. 6 Variation of amplification factor R at the center versus incidence angle α for different values of G with $b/h=0.75$, $2\varepsilon=10$ deg, $k_0b=3.8$ and $(b-a)/\lambda=0.25$

6 Conclusions

The problem of wave oscillation in a circular harbor is analyzed in the presence of a porous wall. For maximum wave dissipation the gap between the porous wall and the harbor wall should be approximately a quarter of the wavelength of the incident waves. A moderate value of the porous-effect parameter G dissipates the maximum wave energy. For a large angle of incidence, wave amplification inside the harbor reduces. The amplification factor depends on the wave number of the incident waves and the location inside the harbor. The amplification factor in the harbor can be adjusted with a proper opening angle and using a porous wall with moderate porosity.

Acknowledgments

This research was sponsored by the Hong Kong Research Grants Council under Grants HKU 568/96E and NSFC/HKU8. The first author was supported financially by a Post-Doctoral Fellowship for the Area of Excellence in Harbor and Coastal Environment Studies.

References

[1] Chwang, A. T., 1998, "Study of Ship Waves in Victoria Harbour," *Proc. 3rd Intl. Conf. Fluid Mech.*, Beijing, China, Beijing Institute of Technology Press, pp. 9–16.
[2] McConnell, K. J., Ethelston, D. M., and Allsop, N. W. H., 1999, "Low Reflection Walls for Harbours: Development of New Structures and Applications in Hong Kong," *Coastlines, Structures and Breakwaters*, N. W. H. Allsop ed., Proc. ICE Breakwaters Conference, London, UK, Mar. 19–20, Thomas Telford, pp. 58–69.
[3] Lamb, H., 1932, *Hydrodynamics*, Dover, New York.
[4] McNown, J. S., 1952, "Waves and Seiches in Idealised Ports," Gravity Waves Symp., National Bureau of Standards, Cir. 521, pp. 153–164.
[5] Kravtchnenko, J., and McNown, J. S., 1955, "Seiche in Rectangular Ports," Q. Appl. Math., **13**, pp. 19–26.
[6] Miles, J., and Munk, W., 1961, "Harbour Paradox," J. Waterways Harbours Div., **87**, No. 3, pp. 111–130.
[7] LeMehaute, B., 1961, "Theory of Wave Agitation in Harbour," J. Hydraul. Div., Am. Soc. Civ. Eng., **87**, No. 2, pp. 31–50.
[8] Ippen, A. T., and Goda, Y., 1963, "Wave Induced Oscillation in Harbours: The Solution for a Rectangular Harbour Connected to the Open Sea," Report No. 59, Hydrodynamics Lab, M.I.T., Cambridge, MA.
[9] Lee, J. J., 1971, "Wave Induced Oscillation in Harbours of Arbitrary Geometry," J. Fluid Mech., **45**, pp. 375–394.
[10] Mei, C. C., and Petroni, R. V., 1973, "Waves in a Harbour With Protruding Breakwaters," J. Waterways, Harbours, Coastal Engrg. Div., **99**, No. 2, pp. 209–229.
[11] Hwang, L. S., and Tuck, E. O., 1970, "On the Oscillations of Harbours of Arbitrary Shape," J. Fluid Mech., **42**, pp. 447–464.
[12] Mei, C. C., and Chen, H. S., 1975, "Hybrid Element Methods for Water Waves," *2nd Annual Symp. of Waterways, Harbour, and Coastal Engrg.*, Vol. 1, ASCE, New York, pp. 63–81.
[13] Chen, H. S., 1986, "Effects of Bottom Friction and Boundary Absorption on Water Wave Scattering," Appl. Ocean. Res., **8**, No. 2, pp. 99–104.
[14] Tsay, T. K., Zhu, W., and Liu, P. L. F., 1989, "A Finite Element Model for Wave Refraction, Diffraction, Reflection and Dissipation," Appl. Ocean. Res., **11**, No. 1, pp. 33–38.
[15] Sollitt, C. K., and Cross, R. H., 1972, "Wave Transmission Through Permeable Breakwaters," *Proc. 13th Conf. on Coastal Engrg.*, Vol. 3, ASCE, Reston, VA, pp. 1827–1846.
[16] Chwang, A. T., 1983, "A Porous Wavemaker Theory," J. Fluid Mech., **132**, pp. 395–405.
[17] Yu, X., and Chwang, A. T., 1994, "Wave-Induced Oscillation in Harbour With Porous Breakwater," J. Waterways, Ports, Coastal Ocean Eng., **120**, No. 2, pp. 125–144.
[18] Lee, M. M., and Chwang, A. T., 2000, "Scattering and Radiation of Water Waves by Permeable Barriers," Phys. Fluids, **12**, No. 1, pp. 54–65.
[19] Williams, A. N., and Li, W., 1998, "Wave Interaction With a Semi-Porous Cylindrical Breakwater Mounted on a Storage Tank," Ocean Eng., **25**, No. 2–3, pp. 195–219.
[20] Chwang, A. T., and Dong, Z., 1984, "Wave Trapping due to a Porous Plate," *Proc. 15th ONR Symp. Naval Hydrodyn.*, National Academy Press, Washington, DC, pp. 407–417.
[21] Yip, T. L., and Chwang, A. T., 2000, "Perforated Wall Breakwater With an Internal Horizontal Plate," J. Eng. Mech., **126**, No. 5, pp. 533–538.
[22] Fugazza, M., and Natale, L., 1992, "Hydraulic Design of Perforated Breakwaters," J. Waterway, Port, Coastal, Ocean Eng., **118**, No. 1, pp. 1–14.
[23] Suh, K. D., and Park, W. S., 1995, "Wave Reflection From Perforated-Wall Caisson Breakwaters," Coastal Eng., **26**, pp. 177–193.